Synthesis and Characterization of Novel Monophasic Hybrid Membranes of Cellulose Acetate by Co-polymerization with Tetraethyl Orthosilicate and 3-(Aminopropyl)triethoxysilane

M. Lopes [a]
[a] Instituto Superior Técnico, Avenida Rovisco Pais, 1, 1049-001, Lisboa, Portugal

*** Corresponding author email address**: miguelalexandrelopes@tecnico.ulisboa.pt

Abstract

Cellulose acetate membranes were one of the pioneer membranes targeted for structural modifications. In this work, membranes of cellulose acetate, silica, and amine, were synthesized by the phase inversion method and sol-gel process, in an acidic medium. Various molar compositions, of unfunctionalized silica and functionalized amine with silica, of 100/0, 95/5, 90/10, 80/20, 70/30 and 50/50 were tested.
Morphological characterization via SEM proves the linear increase in the total membrane thickness with the increase in the molar amine content, and that the silica-amine functionalization did not affect the membranes' skinned asymmetric character. SEM images prove the presence of clusters in the active layer that influence the hydraulic permeability but do not affect the thickness of the membrane. Furthermore, clusters present on the bottom layer have no impact on mechanical properties.
Mechanical properties shows that the Young modulus increases and the rupture elongation decreases as the amine content increases, while the rupture strength remains constant.
Permeation tests reveal an increase in hydraulic permeability with increasing amine content and with decreasing number of clusters and their total area in the active layer. In terms of molecular exclusion rate, it decreases with the introduction of amine. For higher compositions than A90/10 the MWCO increases and then decreases from A80/20 to A70/30, remaining constant afterwards.
Amine functionalization, under pH<5, translates into an increase in hydraulic permeability when compared to cellulose acetate and cellulose acetate and silica membranes. In terms of applicability in blood purification treatments, synthesized amine membranes have great potential.

Keywords: Cellulose Acetate, Silica, Amine, Membrane Functionalization, Sol-Gel

1. Introduction

For the last century populational growth has shown astonishing records of 4.6 to 7 billion people. This crescent growth boosted the accelerated use of separation processes using membranes in many fields of the industry. Cellulose acetate membranes were pioneering and commonly used membranes in ultra and microfiltration processes due to their natural abundance, superior film-forming ability, low price, moderate resistance to chlorinated agents, good biocompatibility, good fouling resistance, and their hydrophilic nature. Furthermore, they played a key role in wastewater treatment plants, gas separation, blood purification and other bioprocesses. However, despite the numerous advantages of pure cellulose acetate membranes, there are some limitations, such as poor mechanical properties and low chemical resistance. Under more adverse operating conditions, such as high temperatures or low pH, the CA (cellulose acetate) polymer hydrolysis occurs, compromising the chemical, physical structure, and thermal stability. To overcome the various limitations imposed by cellulose acetate membranes functionalization appears, then, as an efficient strategy, as it allows the mixture of organic polymer with inorganic materials.

Matrix reinforcement of pure cellulose acetate membranes with silica has been accomplished by the addition of silica nanoparticles. Its synthesis can be done by various techniques such as sol-gel. Hybrid CA-SiO_2 membranes result from two reactions, hydrolysis, and condensation, in that order. The hydrolysis and condensation of silica is achieved by the addiction of a precursor with a silica group, such as TEOS (Tetraethyl Orthosilicate) , in the CA casting solution. The functionalization of cellulose acetate membranes with silica has proven to be an upgrade from the traditional pure cellulose acetate membranes in the most diverse applications. To highlight, there is the application of these hybrid membranes in blood purification treatments. Permeation studies reveal that the integration of silica into CA membranes results in high flux UF (ultrafiltration) membranes with enhanced mass transfer properties, "imitating" the metabolic functions of the kidney. Furthermore, these membranes fully permeated urea and have a total rejection of albumin, while being non-hemolytic, in other words, blood compatible. However, there are some limitations of nowadays membranes in PBUT (Protein Bound Uremic Toxins) filtration in chronic kidney disease and end stage renal disease patients. PBUTs have MW (Molecular Weight) below 500 Da, being very difficult to

remove in dialysis processes due to their great affinity with human blood proteins, with human serum albumin. The non-complete removal, or deficient removal, of these toxic proteins leads to the worsening of the renal patient's condition, and recent studies reveal that PBUT are correlated with increased patient mortality in dialysis treatments.

In this work is presented the synthesis of new hybrid CA/SiO_2, taking advantage of the upgrade of permeation properties, mechanical properties, and applicability to purification treatments of this functionalization, by adding the amine group to the structure of these membranes. Functionalization with NH_2 from the APTES (3-(Aminopropyl)triethoxysilane) precursor reveals to improve the structure of membranes and may be a way to improve the permeation and mechanical properties of CA/SiO_2 membranes. Also, amine is present in numerous biological reactions in the human body and is also present in proteins. This property may be relevant for the removal of toxic components in the blood, particularly in the case of PBUTs.

2. Materials

Casting solutions were prepared using cellulose acetate (~30.000 g/mol) from Sigma-Aldrich, formamide (≥99.5%) from Carlos Erba, acetone (99.7%) from José M. dos Santos, TEOS and APTES (≥98%) from Sigma-Aldrich and nitric acid (>60%) from José M. dos Santos).

Four reference solutes were used to calculate the salts rejection coefficient, being sodium chloride (≥99.5), magnesium chloride hexahydrate (≥99%) and magnesium sulfate heptahydrate (≥99.5%) from Merck, and sodium sulfate (≥99%) from Scharlau S.A.

To obtain the membranes' molecular weight cut-off several polymers were used, such as, PEG 400, 3000, 6000, 10000 and 35000 Da from Merck, PEG 20000 Da from Fulka, and Dextran 40000 Da from Pharmacia Biotech AB).

To the morphological and topographic characterization, membranes were dried with isopropanol (≥99.8%) from Honeywell and n-hexane (≥95%) from Carlos E. Reagents.

3. Membranes synthesis

3.1 *Casting Solutions Preparation*

For the hybrid monophasic membranes, organic content, cellulose acetate, was kept constant (95%wt), and the inorganic content (5%wt), where the molar composition of non-functionalized-silica and amine-functionalized with silica vary. Sol-gel reactions were promoted on plastic reaction vessels at room temperature. The first step comprises the membrane matrix, by adding cellulose acetate and a two-solvent mixture, formamide, and acetone, to promote miscibility. Into this mixture, alkoxide precursors, such as TEOS and APTES were added. To promote hydrolysis/condensation of the alkoxide precursors, DI water, and nitric acid were added too. To achieve a pH media of 2/3, a sample of all casting solutions were tested on dip in pH stripes to know the number of exact drops of nitric acid to be added to the casting solution. Homogenization of the casting solutions was made by magnetic agitator for 24 h and 300 rpm, at room temperature.

Membranes' acronyms and casting solution compositions are exhibited in Table-2 (in annex). Acronyms mirror the membranes' molar composition, as presented in, and reflect the final membranes composition, Table-3 (in annex).

3.2 *Membranes Casting*

After a 24 h period of complete homogenization the casting solution is poured into a gap of the casting knife that is on top of the casting glass. The knife should be dragged vertically from top to bottom, at a controlled and uniform pace, ensuring a rectangular form and absence of accumulation of casting solution on the glass.

Concluding this step, a 30 s evaporation process starts. During this time, acetone (solvent) evaporates from the top of the membrane making the concentration of polymer increase in that area, thus forming the active layer of the casted membrane (in contact with air).

After the 30 s period, the casting glass is poured into a coagulation bath, with DI (Deionized) water at low temperature (between 2-3 ºC), which promotes the solvent exchange with the membrane's matrix and the bath. Between 20 to 30 min membranes begin to self-detached from the glass. At this point, membranes should be marked, with the corresponding nomenclature, at one of the corners of the top layer (layer facing the air), thus, the active layer is signalled. From this, membranes should be stored, in previously washed containers, in cooled DI water at 5 ºC and stored in a refrigerator.

4. Membranes Characterization

4.2 *Morphological and Topographical Studies*

To study the behaviour of the introduction of amine in the CA/SiO_2 membranes, and possible morphological and topographic changes, FEGSEM (Field Emission Gun Scanning Electron Microscope) technique was used and performed by the JM-7001F FEG-SEM (JEOL) equipment at an accelerated voltage of 5.0 kV. Before the technique, membranes were dried and cut into smaller pieces (1cmx1cm), and placed in liquid nitrogen to be cut again, so that the cross section was as uniform as possible. Finally, a film of gold and palladium was deposited on the samples so that they could become electrical conductors, as this image acquisition technique is made at the expense of the incidence of an electron beam. Micrographs of the top surface and bottom layer (magnification of x10000) and cross-sections (magnification of x800) were obtained.

4.3 *Mechanical Properties*

Mechanical properties such as Young modulus, rupture elongation and rupture strength were analysed in a laboratory outside the Instituto Superior Técnico.

5. Evaluation of Permeation Performance

Not knowing the characteristics of hydraulic permeability, salt rejection coefficient and MWCO, the synthesized wet membranes were characterized in an ultrafiltration set-up. The UF is composed by and ISGEV AS71B4 pump coupled to a MOVITRAC LTE SEW EURODRIVE power source, that makes the centrifugal paws rotate and sets the pump position rotating frequency. The feed solution tank, with a capacity for 5 L, it's pumped through the feed line throughout the ultra-filtration five modules, displayed in series. Each UFM (Ultrafiltration Module) has an outlet line or permeate exit. At the end of the UFM set-up there's a manometer. Transmembrane pressure, or TMP (Transmembrane Pressure), and the feed-rate are controlled by a cut-valve and rotameter. The non-permeated solution, or concentrate, goes back to the feed tank through the concentrated line.

UFMs were developed at Instituto Superior Técnico, Lisboa, Portugal, following the original design by Dr. Matsuura and Dr. Souririjan of Ottawa, Canada, National Investigation Council [1]. The UFM permeation area is 13.2 cm^2.

5.1 Membranes Compaction

Compaction, for all tested membranes, was made during 3 hours at 3.0 bar (pressure 20% higher than the maximum pressure used during the permeation experiments) to ensure the formation of uniform rigid pores and a steady permeate flux.

5.2 Hydraulic Permeability

The hydraulic permeability (Lp) represents the membrane's ability to permeate pure water, and is given by the following equation,

$$Lp = \frac{J_{pw}}{TMP} \quad (1)$$

being J_{pw} the flux of permeated water (kg/h m^2), and *TMP* the transmembrane pressure imposed (bar).

Under ultrafiltration conditions, water fluxes were obtained at a feed rate of 150 L/h and a pressure gradient of 0.5, 1, 1.5, 2, and 2.5 bar.

5.3 Salts Rejection Coefficient

The rejection factor can be described as the fraction of solute, present on the feed solution, restrained by the membrane. The definition of rejection factor, *f* is

$$f = \frac{C_f - C_p}{C_f} \quad (2)$$

where C_f and C_p the feed and permeate concentration, respectively, in ppm.

Permeation experiments were carried out at constant pressure and feed-rate (1 bar and 192 L/h respectively).

Salt concentration, on both feed and permeate, was measured by conductivity using a CRISON CONDUCTIMETER GLP 32 having a reproducibility of ±0.1 % and a reading error ≤0.5 %.

5.4 Molecular Weight Cut-Off (MWCO)

The MWCO is the minimum molecular weight, in kDa, where 90% of the solute is rejected by the membrane. For this purpose, polymers with different molecular weights were used to calculate the rejection factor using eq. (2).

Permeation experiments were carried out with equal at constant pressure and feed-rate (1 bar and 192 L/h respectively).

Blank, feed and permeates TOC were measured using a SHIMADZU Total Organic Carbon Analyzer (TOC-V CSH/CSN), working with the combustion chamber at 680 ºC and a reconstituted air pressure of 200 kPa.

5.5 Pore Size

Pore size can be determined by empirical correlations [2] that allow relating the cut-off of a given membrane with the pore diameter (d_p), in nm,

$$dp = 0.09(MWCO)^{0.44}$$

being MWCO in Da.

6. Results and Discussion

6.1 Morphological and Topographical Studies

Membranes synthesized via sol-gel in conjunction with the phase inversion method have two distinct phases: an active layer and a porous layer. Images from SEM shows an active dense top layer and a porous bottom layer in all micrographs, which confirms the integral asymmetric structure and that *in situ* silica and amine-functionalization, CA-SiO_2 and CA-SiO_2-$(CH_3)_3NH_2$ respectively, did not affect the membranes' skinned asymmetric character.

To evaluate the influence of these functional groups on the total membrane thickness (L), cross-section images from were analysed via ImageJ, which is an open-source software for processing of scientific images, to make three measurements of the membranes' thickness, in three different positions, enabling the calculation of an average value and respective standard deviation (std), as shown in the next table.

Table 3-Mean values of membrane thickness, and respective standard deviation, calculated by the ImageJ image analysis program, for the cross-section images at a resolution of x800

Membrane	L (µm)	Std (µm)
A100/0	67	±1
A95/5	53	±0.5
A90/10	53	±1
A80/20	67	±2
A70/30	68	±3
A50/50	88	±1

TEOS/APTES functionalization translates into a 21% decrease in membrane thickness, in the passage from A100/0 to A95/5. This functionalization makes the membrane very dense, that is, there is less spacing of the polymer chains. The increase of the molar composition A95/5 to A90/10 has no structural impact whatsoever, which implies that for this range of compositions the functionalization does not entail changes. For compositions above A90/10, a strictly increasing behaviour of the membrane thickness is noted. From A90/10 to A80/20, from A80/20 to A70/30, and from A70/30 to A50/50, there is a percentage increase of 8%, 19%, and 29%. This is indicative that the increase in the molar APTES content and the decrease in the TEOS content translates into a less dense membrane. This behaviour is expected, since amine functionalization where the casting solution has a pH<5, results in a less dense structure [3]. In this set of results, the least dense membrane corresponds to A95/5 and A90/10, and the densest membrane to A50/50.

Regarding the active layer, the introduction of the functional groups reveals to have a fundamental role in the morphology of the membrane. In all SEM images the presence of white structures/dots can be seen, whose quantity and density varies according to the composition. These structures, from now on, will be called clusters, and will be the target of a more detailed study since the active layer is directly related to hydraulic permeability, rejection of salts and MWCO.

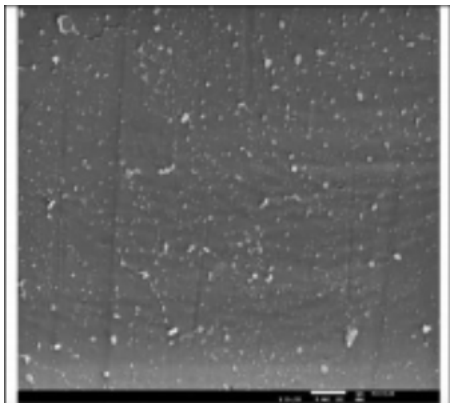

Figure 1-SEM microphotograph of the active at an energy of 15.0 kV and resolution x2000 of A100/0 membrane

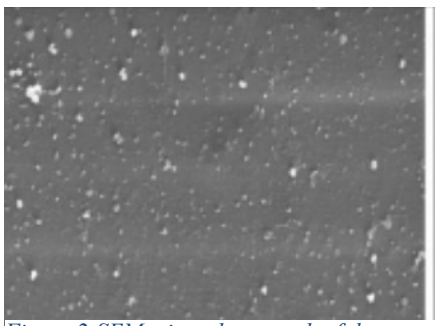

Figure 2-SEM microphotograph of the active at an energy of 15.0 kV and resolution x2000 of A95/5 membrane

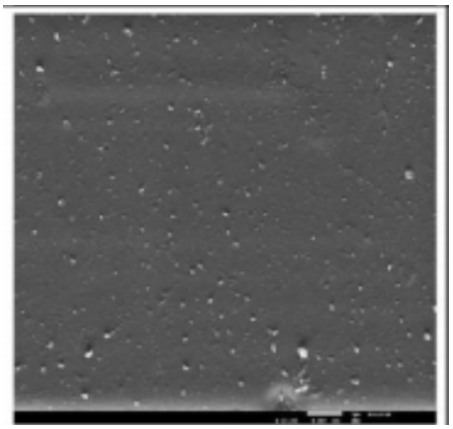

Figure 3-SEM microphotograph of the active at an energy of 15.0 kV and resolution x2000 of A90/10 membrane

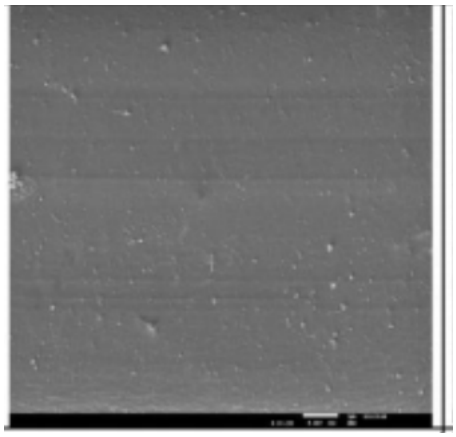

Figure 4-SEM microphotograph of the active at an energy of 15.0 kV and resolution x2000 of A80/20 membrane

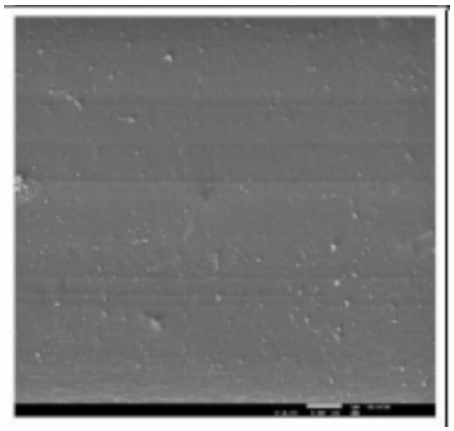

Figure 5-SEM microphotograph of the active at an energy of 15.0 kV and resolution x2000 of A70/30 membrane

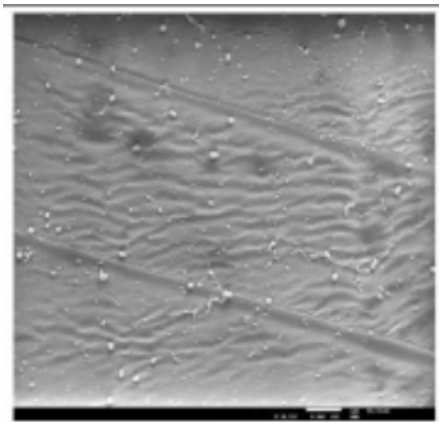

Figure 6-SEM microphotograph of the active at an energy of 15.0 kV and resolution x2000 of A50/50 membrane

In terms of number of clusters in the active layer, figure 7 the introduction of the APTES group does not cause major changes in the morphological levels of the membrane, with a decrease from 2106 to 2045 clusters. With the increase in the amine content and the decrease in the silica group, there is a sharp decrease of 58% in the number of clusters, in the transition from composition A95/5 to A90/10. As the SiO_2-NH_2 group, in molar terms, increases, the number of clusters decreases. From composition 90/10 to 80/20 there is a decrease of 21%, and from 80/20 to 70/30 a decrease of 27%. When the molar content of silica and silica functionalized with amine are equal, 50/50, the number of clusters rises from 495 to 821, translating into an increase of 65%. In global terms, increasing the molar content of NH_2 decreases the number of this structures, except for composition 50/50. Composition A100/0 and A70/30 are the ones with the highest and lowest number of clusters, respectively.

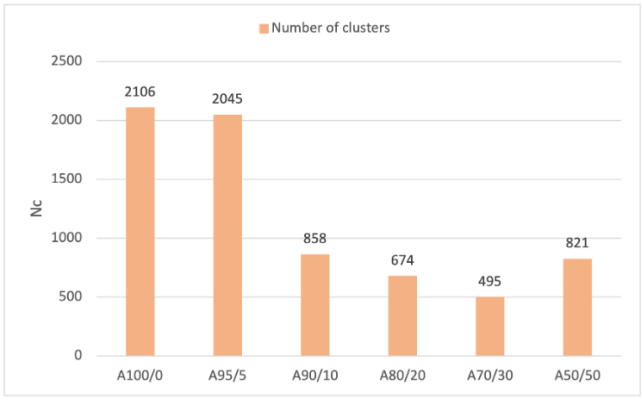

Figure 7-Membranes' number of clusters on the active layer

Figure 8 relates the total area of clusters, that is, the sum of all areas, with the total number of clusters. With the introduction of the APTES precursor, the number of clusters decreases from 2106 to 2045, while the total area increases from 4.3 to 4.5 μm^2. This is indicative that for low amine compositions there will be no noticeable differences. However, from composition A95/5 to A90/10, the number of clusters and the total area, in percentage terms, decreases by 58 and 67%, respectively. This is suggestive that for molar contents above 5%, NH_2 plays a fundamental role in decreasing the number and total area occupied by these structures. This behaviour continues to be verified for compositions above A90/10, except for the A50/50 composition.

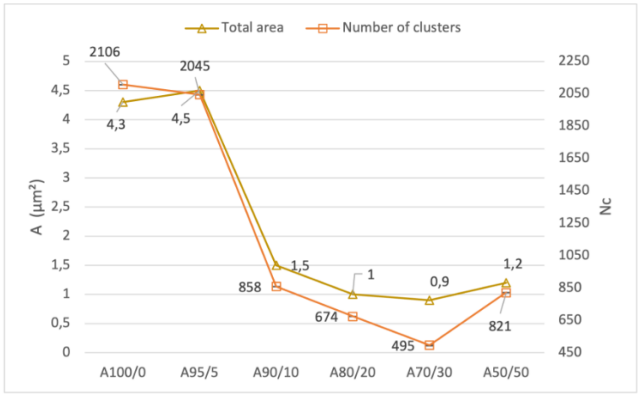

Figure 8-Relationship between the number of clusters and the total area occupied by these structures for the top layer

Regarding the porous layer, figure 9, the total area occupied by the clusters, the behaviour is strictly increasing with the increase of the propylamine group, except for the passage from A70/30 to A50/50. As for the number of clusters, the introduction of the NH_2 group results in a sudden decrease of 57%, with an increase of 106% from A95/5 to A90/10, followed by a strictly decreasing behaviour until the transition from A70/30 to A50/50, where the number of these structures increases. In general, the number of clusters and the area occupied by them decreases with increasing molar content of the APTES precursor, and for TEOS/APTES equimolar compositions, both properties increase. There is a clear deviation from this behaviour, regarding the number of clusters, in the transition from A100/0-A95/5-A-A90/10. This deviation can be explained by the presence of large O-ring-shaped structures in A95/5 membrane which may imply a greater difficulty in the formation of clusters.

Figure 9-Relationship between the number of clusters and the total area occupied by these structures for the bottom layer

6.2 Mechanical Properties

With the introduction of the propylamine group in the functionalized membrane of CA/SiO_2 (A100/0 to A95/5), the Young modulus increases from 53 MPa to 72 MPa. As the molar content of APTES increases, this parameter has a strictly decreasing behaviour, except for A50/50 membrane composition. This behaviour is also verified for rupture elongation, except the first two tested compositions whose value is constant.

Amine functionalization (A95/5) makes the membrane more rigid, this being the highest value obtained for Young modulus for all compositions tested. However, and with the increase of this functional group, the membranes become less rigid. As far as rupture elongation, a higher percentage represents a more ductile material, which implies that as the APTES content increases, membranes become less and less ductile. This set of results allow us to state that the introduction of the amine group in the CA/SiO_2 membranes makes the network more closed, denser, with a much higher elongation at rupture point, while the increase of the NH_2 group the overall network becomes more open, less rigid, elongating less at rupture point [3]. This conclusion is supported with the values obtained for the total membrane thickness, via FEGSEM, as the membranes become less and less dense with the increase of the propylamine group.

The tensile strength results are almost in line with the elongation results. This is expected since for the same Young modulus, the larger is the elongation at rupture point, the larger might be the rupture tensile strength.

Mechanical properties are shown in the following figure.

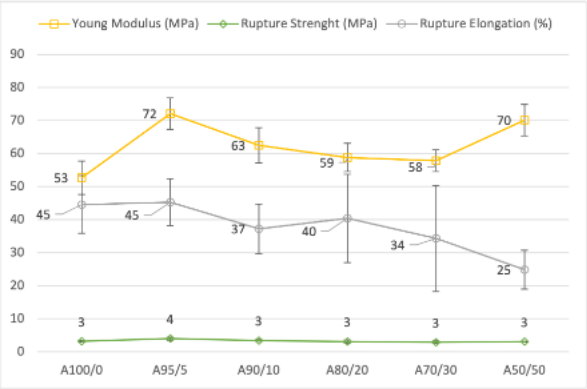

Figure 10-Mechanical properties for the tested membranes

6.3 Permeation Performance

6.3.1 Hydraulic Permeability

Regarding figure 11, hydraulic permeability increases from 42 to 98 kg/(h m^2 bar), in the passage of the pure membrane of CA to A100/0, representing a percentage increase of 133%. This increase it's expected since permeation studies have shown that the integration of silica into CA membranes increases hydraulic permeability [4]. The key factor in changing the behaviour of hydraulic permeability occurs when the propyl-amine group is added to single-phase hybrid membranes. After the introduction of the APTES group, the permeability decreases from 98 to 58 kg/h m^2 bar, representing a 41% decrease in the Lp value. This is due to the complexity of surface chemistry, which now has a variety of species (hydroxyl, acetate, silica, and propyl-amine). In this case, inter-molecular bonds squeeze porous diameter, resulting in the observed decrease. With the increase in the amine content, the hydraulic permeability presents a growing behaviour, with an increase of 26% and 58%, in the passage from A95/5 to A90/10, and from A90/10 to A80/20, respectively. This suggests that for these ranges of compositions, the additional disorder caused by the propyl-amine chains is sufficient to force the opening of the overall network, producing more empty spaces, which justifies the increase in permeability. Concerning the three final compositions, the hydraulic permeability value tends to stabilize, although there is a small decrease of 14% from A80/20 to A70/30. For this range of molar compositions, hydraulic permeability is (111±11) kg/h m^2 bar.

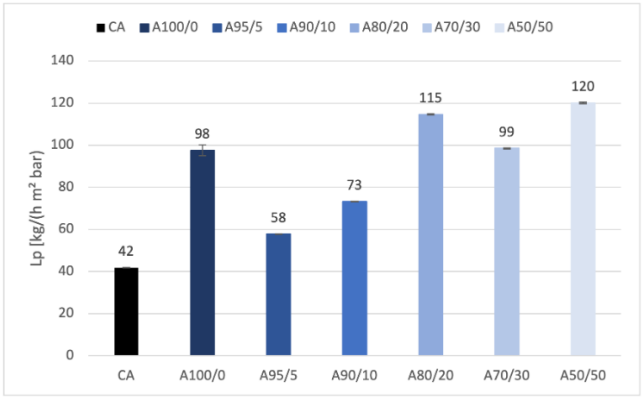

Figure 11-Hydraulic Permeability for the tested membranes

Interestingly, the behaviour observed is opposite to that reported in published works. The following figure compares the values obtained in the current work against the values obtained by other authors [3]. It is important to mention that the membranes, when compared, have the same composition.

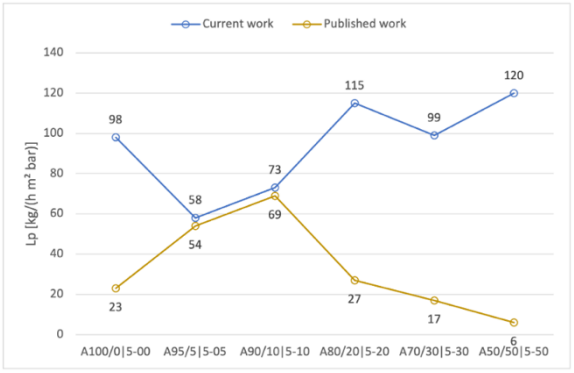

Figure 12-Comparison of the behaviour, of current work with published work, of the hydraulic permeability for monophasic hybrid membranes

By analysing figure 12 there is a big difference between the works regarding hydraulic permeability behaviour. This noticeable difference is due to the pH of the casting solution. In the current work, the amount of nitric acid added was such as to reach a pH 2/3 for all the synthesized compositions. In the published work, the number of drops added for the CA/TEOS membrane, 5-00, was six, and for the remaining compositions of CA-SiO_2-NH_2 membranes was nine. The type of structure formed by the membrane to be synthesized depends on the balance between the hydrolysis and condensation steps, which are strongly affected by the pH of the casting solution. For acidic conditions (pH<5) condensation only occurs after all the precursors are hydrolysed. Thus, an extensive branching and therefore more open, less dense 3D network is produced since most functional groups -OH are available for condensation[3]. For more basic media (pH>10), hydrolysis and condensation happen at the same time, with fewer -OH groups being available for the condensation step, resulting in linear, less branched, and denser structures.

For membranes with only TEOS (A100/0 and 5-00), there is a standard deviation of ±53 kg/h m^2 bar between the two values. This is suggestive that the number of drops added to the casting solution, in the published work, was not enough to reach a pH<5, implying a much denser structure when compared to A100/0, justifying the difference in hydraulic permeability values.

With the introduction of propyl-amine in the membrane structure, Lp decreases in current work, and increases in published work, with a standard deviation of ±3 kg/h m^2 bar between A95/5|5-05 and A90/10|5-10. The similarity between the values of hydraulic permeability suggests that the number of drops added in the published work, six, was enough to reach a pH<5, and close to the pH of the current work. For the last compositions there is a standard deviation of ±62, ±58, and ±81 kg/h m^2 bar for A80/20|5-20, A70/30|5-30, and A50/50|5-50, respectively. In the current work, with the increase of the APTES group, the amount of acid drops added to the casting solution also increased to reach a pH=2/3.This is indicative that, for molar compositions greater than 90/10, there will be a greater difficulty in protonating the amine group, since there are a greater number of NH_2 groups that can capture the H^+ ions in solution. In the published work, the number of drops added was six, as mentioned above. Keeping the number of drops equal, as the amine content increases, there will be more and more NH_2 groups available to capture ions, making the pH of the casting solution higher as the molar content of APTES increases. Consequently, for the published work, the pH reached will be close to, or higher than 10, which implies in increasingly dense structures, with the increase of NH_2, causing the linear decrease observed in the hydraulic permeability behaviour. This is not verified in the current work.

6.3.2 Salts Rejection Coefficient

The results obtained for the rejection coefficients, at 1 bar and 180 L/h, are presented in the following figure.

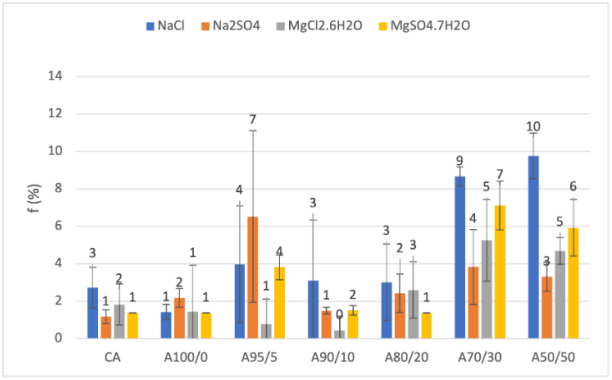

Figure 13-Rejection factor for reference salts

For the pure cellulose acetate membrane, NaCl presents the highest rejection factor, 3%, followed by $MgCl_2$, 2%, and finally Na_2SO_4 and $MgSO_4$ both with a rejection of 1%. With the introduction of the silica group, the rejection factor for NaCl decreases from 3% to 1%, $MgCl_2$ from 2% to 1%, while the rejection of Na_2SO_4 increases from 1% to 2% and that of $MgSO_4$ remains unchanged. Although the CA/TEOS functionalization promotes higher permeate salt fluxes, the rejection coefficient does not show major changes, meaning that the introduction of SiO_2 and respective structural and morphological changes caused in pure CA membranes, do not impact this property.

The shifting point of the "stationary" behaviour of the rejection coefficients changes with the introduction of the APTES group. When changing the molar composition from A100/0 to A95/5, the rejection coefficients increase by 3\% for NaCl, Na_2SO_4 and $MgSO_4$ while $MgCl_2$ remains unchanged. When changing from A100/0 to A95/5, the rejection coefficients increase by 3% for NaCl, Na_2SO_4 and $MgSO_4$ while $MgCl_2$remains unchanged. With the increase of the amine molar composition, from A95/5 to A90/10, the rejection factor decreases to 3%, 2%, 1%, and 0%, for NaCl, $MgSO_4$, Na_2SO_4, and $MgCl_2$, respectively. Between A90/10 and A80/20 molar compositions, rejection coefficients do not show great changes, except $MgCl_2$ which shows an increase from 0% to 3%. When the amine content increases again, A70/30, all rejection coefficients increase, remaining stable for higher molar compositions, A50/50.

Due to the dimensions of the salts in solution, all membranes are permeable to the reference salts.

6.3.3 MWCO

The following figure shows the MWCO for the tested compositions.

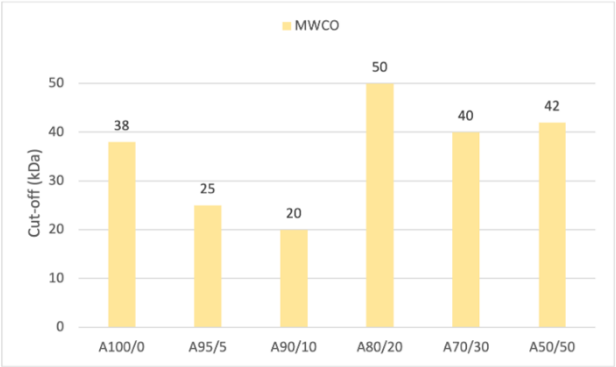

Figure 14-MWCO of the tested membranes

When going from A100/0 to A95/5, and from A95/5 to A90/10, there is a decrease of 34% and 20% in the MWCO. This decrease is to be expected, since the increase in the SiO_2 content in the CA matrix promotes the increase in MWCO [5]. In this case, and for this set of compositions, the molar reduction of the TEOS group promotes a decrease in the value of this property. Furthermore, for molar compositions A95/5 and A90/10, the APTES group does not make a visible contribution, as the decreasing behaviour seen depends on the decrease of silica. The "turning point" is from the A80/20 composition, as there is a notorious 150% increase in the MWCO value, from A90/10 to A80/20. This increase suggests that, despite the silica content and theoretically the MWCO value should also decrease, the molar content of APTES group introduced is sufficient to counteract this decrease. Once again, functionalization of CA-SiO2 membranes with NH_2 shows the amine's potential. However, and for compositions above A80/20, MWCO decreases, and tends to stabilize between 40 and 42 kDa. Like what happened in the above-mentioned references, starting from a given silica composition the MWCO would have a maximum value, which would decrease with the increase of the silica content. This can be indicative that for compositions around A80/20, the MWCO value will be maximum, and that for higher compositions of amine, the value tends to decrease. Despite what was mentioned, the MWCO stabilizes after the maximum value recorded, even with the increase in NH_2 and decrease in SiO_2 which suggests that for this range of compositions, the MWCO cut-off is not affected.

All synthesized membranes have a strong potential for the filtration of human blood, especially PBUTs. These toxic uremic proteins have a molecular weight <500 Da which theoretically implies that they are permeated by membranes since the cut-off is greater than their molecular weight. On the other hand, these PBUTs are tightly bound, through ionic and/or hydrophobic characteristics, to albumin in the blood. Since albumin has a molecular weight of 60 kDa, all membranes would reject this protein, which is desired. However, it is necessary to test whether the amine group will intervene and break this strong bond between PBUT-Albumin, which is only possible through permeation tests to these toxins. These set of affirmations are mere hypotheses.

6.3.4 Pore Size

The following figure encompasses the results obtained.

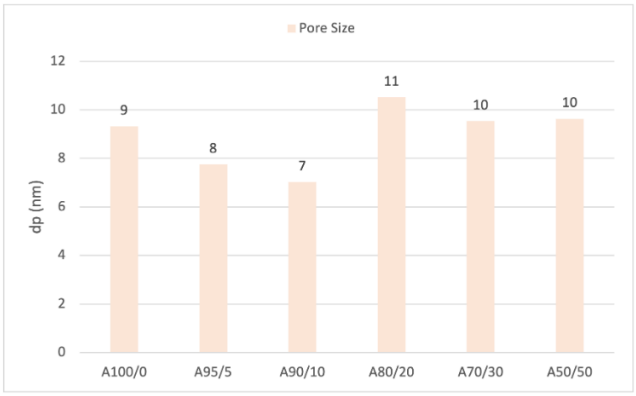

Figure 15-Pore diameter of the tested membranes

By analysing the figure above, the reduction of the SiO_2 group and the introduction of the NH_2 group promotes a linear decrease in pore size. However, for higher amine contents, A80/20, the pore size increases, remaining stable for higher compositions, showing the amine functionalization alters the properties of the membrane, since in this same range it is where the increase, and the highest values, of hydraulic permeability are registered. All synthesized membranes have typical pore diameter values for UF membranes, ranging from 2 to 50 nm.

Conclusions

Pure cellulose acetate membrane, cellulose acetate silica membrane and amine functionalized silica and cellulose acetate membranes were prepared and synthesized by the phase inversion method. Silica and amine were added to the cellulose acetate polymer matrix, *in-situ,* via the sol-gel process, by the addition of precursors, TEOS (silica precursor) and APTES (amine precursor), so that the process of hydrolysis and condensation would occur, to promote the chemical bond between silica and amine with the polymer.

Morphological and topographic analysis via FEGSEM allowed us to conclude that the functionalization of CA/SiO_2 membranes with amine leads to a linear increase in the total membrane thickness with the increase in the molar content of the amine, once for conditions of pH<5 condensation only occurs after total hydrolysis of the precursors, which implies extensive branching and less dense/compact structures. Images of the active and bottom layers reveal the presence of clusters in all membranes functionalized with SiO_2 and SiO_2-NH_2. Regarding the top layer, the number of clusters remains stable for reduced molar amine contents, A100/0 and A95/5, drastically reducing for higher molar

compositions. This behaviour repeats for the total area of these structures. Concerning the bottom layer, the number of clusters and the area occupied by them decreases with increasing molar content of the APTES precursor, and for TEOS/APTES equimolar compositions, both properties increase. There is a clear deviation from this behaviour, regarding the number of clusters, in the transition from A100/0-A95/5-A-A90/10. This deviation can be explained by the presence of large O-ring-shaped structures in A95/5 membrane. Images of the cross sections allowed the identification of two layers: the active dense layer (top layer) and a porous layer (bot layer). Functionalization with the APTES precursor reveals that there is no kind of interference in the asymmetrical character in the synthesized membranes.

In terms of mechanical properties, with the introduction of the propylamine group in the functionalized membrane of CA/SiO_2 (A100/0 to A95/5), the Young modulus increases from 53 MPa to 72 MPa. As the molar content of APTES increases, this parameter has a strictly decreasing behaviour, except for A50/50 membrane composition. This behaviour is also verified for rupture elongation, except the first two tested compositions whose value is constant. Tensile strength results are almost in line with the elongation results. This is expected since for the same Young modulus, the larger is the elongation at rupture point, the larger might be the rupture tensile strength. Generally speaking, as the amine content increases, membranes become less rigid and less ductile. Furthermore, clusters present on the bottom layer do not explain any variations on the mechanical properties.

Regarding the permeation of pure water, when compared to the pure cellulose acetate membrane, the introduction of silica in the membrane matrix translates into a 133% increase in the hydraulic permeability value, as expected. The introduction of the NH_2 group in the CA/SiO_2 matrix translates into a 41% decrease in the Lp value, revealing that the chemical complexity of the membrane surface is such that it negatively affects this permeation property. However, with increasing molar amine content, there is an increase of 26% and 58% from A95/5 to A90/10, and from A90/10 to A80/20. For higher molar compositions, hydraulic permeability values tend to stabilize. The determination of the Lp value reveals that the functionalization with the APTES precursor results in an improvement of the hydraulic permeability when compared to the pure CA and CA/SiO_2 membrane. When CA/SiO_2/NH_2 membranes are compared with published result values, it is concluded that the pH of the casting solution has a direct impact on the permeation properties. For casting solutions at pH<5, the Lp value is favoured, while for more basic pH, the three-dimensional mesh structures produced are more compact, which leads to a decrease in the hydraulic permeability value with an increase in the molar content of NH_2. When the values of Lp, in the present work, are related to the properties of the clusters, there is a tendency for an increase in permeability with a decrease in the number of these structures and a decrease in the total area occupied by them, as the NH_2 increases.

About the rejection of reference salts, the membranes are permeable, an expected result since UF membranes are permeable to mono and divalent salts. There is no behaviour that explains the increase or decrease in the rejection of salts, but, in general terms, the rejection coefficients tend to increase with the increase in the molar amine content, and that the molecular weight of the salts has no effect on this permeation property.

In determining the molecular exclusion rate for a 90% rejection, the introduction of the amine group reveals itself in a decrease in the MWCO of the membranes, which decreases from 38 to 25 kDa, and from 25 kDa to 20 kDa, between A100/0 for A95/5 and from A95/5 to A90/10, respectively. When the molar amine composition is greater than A90/10, the cut-off MWCO increases by 150%, then decreases by 20% from A80/20 to A70/30. From A70/30 onwards, the value of this property stabilizes.

Through empirical correlations it was possible to estimate the pore size of the membranes. There is a linear decrease in pore size between compositions A100/0 and A90/10. However, pore size increases considerably to A80/20, and remains constant for higher compositions.

In summary, amine functionalization of membranes under pH<5 conditions translate into an increase in hydraulic permeability when compared to traditional cellulose acetate membranes and cellulose acetate and silica membranes. These membranes, in addition to the high permeation fluxes, permeate reference salts. In terms of applicability, particularly in blood purification treatments, synthesized membranes have great potential. However, in terms of mechanical properties, membranes are less rigid, and elastomer than CA/SiO_2/NH_2 membranes synthesized in basic media.

References

[1] A. R. Costa and M. N. de Pinho, “Performance and cost estimation of nanofiltration for surface water treatment in drinking water production,” *Desalination*, vol. 196, no. 1–3, pp. 55–65, 2006, doi: 10.1016/j.desal.2005.08.030.

[2] S. Lentsch, P. Aimar, and J. L. Orozco, “Separation albumin–PEG: Transmission of PEG through ultrafiltration membranes,” *Biotechnol. Bioeng.*, vol. 41, no. 11, pp. 1039–1047, 1993, doi: 10.1002/bit.260411106.

[3] M. C. Andrade, J. C. Pereira, N. de Almeida, P. Marques, M. Faria, and M. C. Gonçalves, “Improving hydraulic permeability, mechanical properties, and chemical functionality of cellulose acetate-based membranes by co-polymerization with tetraethyl orthosilicate and 3-(aminopropyl)triethoxysilane,” *Carbohydr. Polym.*, vol. 261, p. 117813, 2021, doi:

https://doi.org/10.1016/j.carbpol.2021.117813.

[4] M. Faria, C. Moreira, T. Eusébio, P. Brogueira, and M. N. de Pinho, "Hybrid flat sheet cellulose acetate/silicon dioxide ultrafiltration membranes for uremic blood purification," *Cellulose*, vol. 27, no. 7, pp. 3847–3869, 2020, doi: 10.1007/s10570-020-02985-2.

[5] G. Mendes, "Novas Membranas Assimétricas de Matriz Mista de Acetato de Celulose e Sílica," 2016.

Annex

Table 1-Membranes' acronyms and casting solution massic composition

Acronyms/Compounds	CA	A100/0	A95/5	A90/10	A80/20	A70/30	A50/50
CA	16.40	16.40	16.40	16.40	16.40	16.40	16.40
Formamide	29.00	29.00	29.00	29.00	29.00	29.00	29.00
Acetone	51.10	51.10	51.10	51.10	51.10	51.10	51.10
TEOS	-	3.00	2.85	2.70	2.40	2.10	1.50
APTES	-	0.00	0.16	0.32	0.64	0.96	1.60
DI water	-	0.5	0.5	0.5	0.5	0.5	0.5
HNO_3	-	3-4 drops	2 drops	8 drops	12 drops	19-20 drops	33 drops
pH	-	2-3					

Table 2-Acronym's designation based on the membrane's molar composition (%)

Acronyms	CA	100/0	95/5	90/10	80/20	70/30	50/50
CA	0.032	0.032	0.032	0.032	0.031	0.031	0.031
SiO_2	0.000	0.830	0.790	0.750	0.660	0.580	0.410
SiO_2-$(CH_2)_3NH_2$	0.000	0.000	0.042	0.082	0.166	0.248	0.410
SiO_2 + SiO_2-$(CH_2)_3NH_2$	0.000	0.830	0.832	0.832	0.826	0.828	0.820
Non-functionalized-SiO_2 /Total SiO_2 (i.e. TEOS/TEOS+APTES)	0.000	100	95	90	80	70	50
Amine-functionalized silica /Total SiO_2 (i.e. APTES/TEOS+APTES)	0.000	0.00	5	10	20	30	50